

C-Terminal End of Aquaporin 0 Regulates Lens Gap Junction Channel Function

Kulandaiappan Varadaraj, Junyuan Gao, Richard T. Mathias, and Sindhu Kumari

Physiology and Biophysics, Renaissance School of Medicine, Stony Brook University, Stony Brook, New York, United States

Correspondence: Kulandaiappan Varadaraj, Department of Physiology and Biophysics, Renaissance School of Medicine, Stony Brook University, Stony Brook, New York 11794-8661, USA; kulandaiappan.varadaraj@stonybrook.edu.

Submitted: February 4, 2019

Accepted: May 9, 2019

Citation: Varadaraj K, Gao J, Mathias RT, Kumari S. C-terminal end of aquaporin 0 regulates lens gap junction channel function. *Invest Ophthalmol Vis Sci.* 2019;60:2525-2531. <https://doi.org/10.1167/iovs.19-26787>

PURPOSE. We reported previously that aquaporin 0 (AQP0) modulates lens fiber cell gap junction (GJ) channel function. The present study was conducted to find out whether the C-terminal end of AQP0 is involved in this regulation.

METHODS. A mouse model, AQP0^{ΔC/ΔC}, was genetically engineered to express AQP0 with 1-246 amino acids, without the normal intact AQP0 (1-263 amino acids) in the lens. Transparency and focusing of the lens were assessed. Intracellular impedance was measured to determine GJ coupling resistance. Intracellular hydrostatic pressure (HP) was also determined. Western blotting was performed to determine connexin (Cx46 and Cx50) expression levels.

RESULTS. At postnatal day 10, AQP0^{ΔC/ΔC} mouse lenses relative to age-matched wild-type lenses showed loss of transparency and abnormal optical distortion; GJ coupling resistance increased in the differentiating (1.6-fold) and mature (8-fold) fiber cells; lens HP increased approximately 1.5-fold at the junction between the differentiating and mature fiber cells and approximately 2.0-fold in the center; there was no significant change ($P > 0.05$) in expression levels of Cx46 or Cx50.

CONCLUSIONS. The increase in GJ coupling resistance was not associated with reduced connexin expression, suggesting either a reduction in the open probability or some physical change in plaque location. The increase in resistance was significantly greater than the increase in HP, suggesting less pressure-driven water flow through each open GJ channel. These changes may lead to a loss of transparency and abnormal optical distortion. Overall, our data demonstrate the C-terminal end of AQP0 is involved in modulating GJ coupling to maintain lens transparency and homeostasis.

Keywords: aquaporin 0, C-terminal end-cleaved AQP0, gap junction coupling, intracellular hydrostatic pressure, lens transparency

The mammalian lens is a transparent and avascular organ that focuses light coming from an object onto the retina. The lens has a single layer of cuboidal anterior epithelial cells with actively proliferating equatorial cells. Proliferating equatorial cells give rise to secondary fiber cells that elongate to form the bulk of the lens. Older fiber cells are internalized as new layers are added over older cells.

During the differentiation of the fiber cells, aquaporin 0 (AQP0), a membrane water channel protein containing 263 amino acids, begins to express at the outer cortex. As the fiber cells elongate and mature, they eliminate cellular organelles as these structures would scatter light.¹ AQP0 undergoes gradual loss of N- and C-terminal ends as a posttranslational modification and as part of fiber cell remodeling.^{2,3} These alterations reduce light scattering and aid the central fiber cells to survive throughout life. AQP0 is a low-permeability water channel⁴⁻⁹ and a cell-to-cell adhesion (CTCA) molecule.^{3,10-15} It is the predominant membrane protein (45%) in the fiber cells.¹⁶ The functions of AQP0 are critical for maintaining lens transparency,^{8,11,12,17} refractive index gradient,^{8,17,18} biomechanics,¹⁹ and homeostasis.^{4,7,8,11,12,17-19} There are protein-protein interactions of AQP0 with connexins;^{13,20-22} with lens-specific cytoskeletal beaded filament proteins,²³ CP49 (phakinin) and filensin (CP115);²⁴ and with

crystallins.^{25,26} AQP0 and the above-mentioned interacting proteins undergo a gradual loss of N- and C-terminal ends. The C-terminal end-cleavage starts at the inner cortex; the amount of end-cleaved forms increases toward the outer nucleus, and the inner nucleus contains only the end-cleaved forms.^{2,18,27,28} End-cleavage has been speculated to be part of the aging process; however, N- and C-terminal end-cleavage occurs even in the lenses of 2-year-old humans²⁷ and postnatal day 10 (P10) mice pups.¹⁷ These types of cleavages are accelerated at old age in human lenses.^{2,28}

Connexin (Cx) transmembrane proteins form gap junction (GJ) channels between the fiber cells, allowing small molecules such as ions (Na⁺ and Ca²⁺), cellular metabolites, and second messengers to move between cells.²⁹⁻³⁸ Epithelial cells express Cx43 and Cx50, whereas fiber cells express Cx46 and Cx50.³⁹ AQP water channels are present in epithelial and fiber cells.⁴⁰⁻⁴³ AQP1 and AQP5 are expressed in the epithelial cells, and AQP0 and AQP5 in the fiber cells. All play important roles in the lens microcirculation and homeostasis. Alterations or loss of AQP0, Cx46, or Cx50 lead to loss of homeostasis and lens opacities.⁴³⁻⁴⁶ Several mutations in AQP0 or GJ proteins are responsible for congenital cataracts.^{44,45}

The avascular lens has developed a unique internal microcirculation for homeostasis. The microcirculation facili-

tates ion and nutrient to enter and metabolic waste to exit the lens; AQP0s, GJs and ion channels (transporters, cotransporters, and exchangers) are involved in creating and maintaining the microcirculation.^{38,46-48} The lens microcirculation model proposed by Mathias et al.^{38,46} suggests that sodium ions enter at the anterior and posterior poles and move through the extracellular space toward the center of the lens. Extracellular sodium moves toward the center of the lens because the sodium ions are continuously leaving the extracellular compartment as they enter fiber cells down their transmembrane electrochemical potential. In the intracellular compartment, a center-to-surface electrochemical gradient develops to drive sodium ions through GJs toward the equatorial surface where they are transported out by the epithelial $\text{Na}^+\text{-K}^+\text{-ATPases}$ (for Na^+) or $\text{Na}^+/\text{Ca}^{2+}$ exchanger and $\text{Ca}^{2+}\text{-ATPase}$ (for Ca^{2+}). Osmosis drives water flow to follow the sodium flow and enter fiber cells across their cell membranes. In the intracellular compartment, salt and water both flow through GJs, so osmosis is not possible; instead, a center-to-surface hydrostatic pressure (HP) gradient develops to drive water flow through GJs to the lens surface. At the lens surface, the fluid follows the sodium and leaves the lens due to transmembrane osmosis. In this microcirculation, the inward fluid flow carries nutrients and antioxidants to central fiber cells, while the outward fluid flow carries waste products from central fibers to surface epithelial cells. GJs are involved in the outflow of the lens microcirculatory system.³⁹ Measurement of the intracellular HP gradient provides information on the number of open GJ channels conducting the radial flow of both sodium and water and also indicates the functional state of the sodium circulation.

Atomic force microscopy (AFM) studies showed that end-cleaved AQP0 in the mature fiber cells regulates the spatial localization of GJs.^{49,50} Modulation of GJs by AQP0 has been reported by in vitro investigations.^{13,51} We demonstrated that AQP0, in the presence of lens beaded filament proteins, modulates GJ channel function²⁴ and suggested that fiber cell-to-fiber cell adhesion by AQP0 could be a significant factor in the regulation of GJ function. To understand the role of the C-terminal end of AQP0 in the lens physiology, we developed a mouse model, $\text{AQP0}^{\Delta\text{C}/\Delta\text{C}}$, that expresses only end-cleaved AQP0 in the fiber cells.¹⁷ Lenses of these mice developed cataracts by P15, so we studied lenses at P10 to see what physiological changes preceded the formation of cataracts and thus might be causal. GJ coupling resistance and HP were measured in age-matched wild-type (WT) and $\text{AQP0}^{\Delta\text{C}/\Delta\text{C}}$ lenses.

MATERIALS AND METHODS

Animals

WT C57BL/6J (C57; Jackson Laboratories, Bar Harbor, ME, USA) and the C-terminal end-cleaved AQP0-expressing knockin mouse model¹⁷ $\text{AQP0}^{\Delta\text{C}/\Delta\text{C}}$ were used. Animal procedures were performed according to the ARVO Statement for the Use of Animals in Ophthalmic and Vision Research, the National Institutes of Health's (Bethesda, MD, USA) Guide for the Care and Use of Laboratory Animals, and protocols approved by the Stony Brook University Animal Care and Use Committee.

WT and $\text{AQP0}^{\Delta\text{C}/\Delta\text{C}}$ were genotyped to confirm the absence of the natural mutation in CP49 gene, which was identified originally in mouse 129 strains.⁵² Genomic PCR was done using the primers and protocols as described previously.^{17,52} Development and characterization of the $\text{AQP0}^{\Delta\text{C}/\Delta\text{C}}$ mouse were described recently.¹⁷

Evaluation of Lens Transparency and Aberration

Lens transparency was assessed as described by Kumari et al.²⁴ In short, P10 lenses of WT and $\text{AQP0}^{\Delta\text{C}/\Delta\text{C}}$ mice were dissected and placed into mammalian physiological saline (37°C). Lens imaging of WT and $\text{AQP0}^{\Delta\text{C}/\Delta\text{C}}$ was done under the same lighting and imaging conditions, using a dark-field binocular microscope with a digital camera. Aberrations in the lens were qualitatively evaluated using dark-field optical grid focusing. Each lens was placed on a copper electron microscope specimen grid and imaged. Light scatter and aberrations were assessed by the quality of the grid lines focused by the lenses.

Lens GJ Coupling Measurement

Lenses were dissected from P10 WT and $\text{AQP0}^{\Delta\text{C}/\Delta\text{C}}$ pups and mounted as described by Gao et al.⁵³ and Kumari et al.²⁴ For each impedance study, the lens was mounted in the perfusion chamber that was attached to a microscope stage and perfused with normal Tyrode's solution.

GJ coupling resistance (intracellular impedance) was measured using microelectrodes filled with 3M KCl with initial resistances of 1.5 to 2 megaohms (M Ω).⁵⁴ A microelectrode was inserted into a central fiber cell, and a wide-band stochastic current was injected. Another microelectrode was inserted into a peripheral fiber cell at a distance r (cm) from the center of a lens of radius a (cm) to record the induced voltage. The frequency domain impedance (induced voltage \div injected current) of the lens was recorded in real time using a fast Fourier analyzer (Hewlett Packard, Palo Alto, CA, USA). At high frequencies, the magnitude of the lens impedance asymptotes to the series resistance (R_s), which is the resistance of all the GJs between the point of voltage recording and the surface of the lens. R_s (kiloohms [K Ω]) was measured at multiple depths in lenses of WT and $\text{AQP0}^{\Delta\text{C}/\Delta\text{C}}$ mice; curve fitting of the data with Equation 1 was done to determine the underlying effective intracellular resistivities (R_{DF} and R_{MF} K Ω /cm). These are directly proportional to the radial component of GJ coupling resistance.

$$R_s(r) = \begin{cases} \frac{R_{DF}}{4\pi} \left(\frac{1}{r} - \frac{1}{a} \right) & b \leq r \leq a \\ \frac{R_{DF}}{4\pi} \left(\frac{1}{b} - \frac{1}{a} \right) + \frac{R_{MF}}{4\pi} \left(\frac{1}{r} - \frac{1}{b} \right) & 0 \leq r \leq b \end{cases} \quad (1)$$

Peripheral differentiating fibers (DF; outer cortex containing intact proteins) transition to central mature fibers (MF) at a radial location $b \cong 0.85a$, where r (cm) is the radial distance from the lens center and a (cm) the lens radius. MF area includes inner cortex and outer nucleus (both containing mature fiber cells that have undergone posttranslational modifications), both of which have eliminated intracellular organelles and contain modified membrane proteins. The C-termini of Cx46 and Cx50 are cleaved at the transition from DF to MF, resulting in a coupling resistance change. From the effective resistivities, the GJ coupling conductance per area of cell-to-cell radial contact can be estimated by:

$$G_{DF,MF} = \frac{1}{wR_{DF,MF}} \frac{S}{\text{cm}^2}, \quad (2)$$

where we assume $w \cong 3 \times 10^{-4} \text{cm}$ is the fiber cell width.

Lens Intracellular HP Measurements

Lenses from P10 WT and $\text{AQP0}^{\Delta\text{C}/\Delta\text{C}}$ pups were dissected, and intracellular HP in intact lenses was quantified as described by Gao et al.⁵⁵ and Kumari et al.²⁴ Briefly, microelectrodes of 1.5- to 2-M Ω resistance range were pulled and filled with 3M KCl and gently inserted into the intact lens. The cytoplasm forced into the microelectrode tip due to the positive intracellular

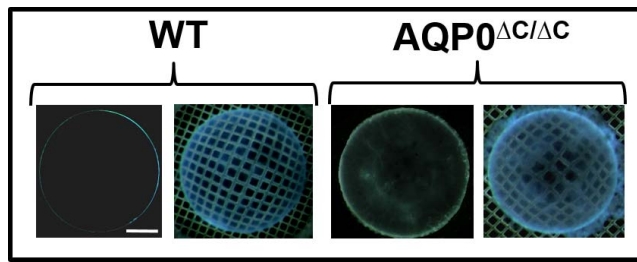


FIGURE 1. Comparison of lens transparency and optical distortion in WT and AQP0^{ΔC/ΔC} mouse lenses at age P10. In all the lenses, a thin layer of light scattering was observed from the capsule and the anterior epithelial cells. At P10, AQP0^{ΔC/ΔC} mouse lenses show reduced transparency with higher levels of light scattering compared to WT. Lenses were imaged with anterior pole facing up. Lenses of AQP0^{ΔC/ΔC} mice focusing the electron microscopy grid show increased barrel distortion compared to the WT lens.

pressure of the fiber cell causes an increase in resistance. The pressure was applied to the interior of the microelectrode until its resistance returned to the value measured outside of the lens. A manometer was used to measure the pressure applied to the microelectrode. Intracellular pressure was measured at four to five depths for each lens. For each genotype, data from at least eight lenses were pooled. By curve-fitting Equation 3 to the pooled data, the average pressure gradient was estimated.

$$p_i(r) = \begin{cases} p_i(b) \left(\frac{a^2 - r^2}{a^2 - b^2} \right) & b \leq r \leq a \\ p_i(b) + (p_i(0) - p_i(b)) \left(\frac{b^2 - r^2}{b^2} \right) & 0 \leq r \leq b \end{cases} \quad (3)$$

The quadratic r -dependence of pressure suggests the transmembrane entry of water into fiber cells is essentially uniform with depth into the lens.⁵³ The change in the slope of the r -dependence at $r = b$ is thought to occur because the number of open GJ channels is different in the MF relative to DF.

Western Blotting

Fiber cell membrane proteins of WT and AQP0^{ΔC/ΔC} lenses were isolated by extraction with 4M-urea buffer (4 mM Tris-HCl, pH 8.0; 5 mM EDTA, 4M-urea). Western blotting was done as previously described.^{11,17} Antibodies to Cx46 and Cx50 (Santa Cruz Biotechnology, Inc., Dallas, TX, USA) were used. Immunoreaction to an antibody was detected using an alkaline phosphatase kit (Vector Laboratories, Inc., Burlingame, CA, USA).

Statistical Analysis

Student's t -test was performed using a statistical software (SigmaPlot 10; Systat Software Inc., San Jose, CA, USA). P values ≤ 0.05 were considered significant.

RESULTS

Lens Transparency and Focusing

We imaged WT and AQP0^{ΔC/ΔC} mouse lenses at P10, under the dark field, to assess transparency. Compared to age-matched WT lenses, AQP0^{ΔC/ΔC} lenses showed a reduction in transparency and changes in optical distortion (Fig. 1). No cataract was evident at P10 lenses of AQP0^{ΔC/ΔC} mice. The electron microscopy grid pattern magnified by WT lenses produced a barrel deformation, called positive barrel distortion aberration, throughout. In this deformation, the straight lines curve inward

TABLE 1. AQP0^{ΔC/ΔC} Lens Fiber Cell GJ Coupling Conductances, Regional Values of Resistivity, and Normalized Coupling Conductance of WT and AQP0^{ΔC/ΔC} Lenses

Genotype	Zone	R_i , K Ω -cm	G_i , S/cm ²	Fold Decrease of G_i
WT	DF	2.2678	1.4699	-
WT	MF	0.6436	5.1792	-
AQP0 ^{ΔC/ΔC}	DF	3.6529	0.9125	1.60*
AQP0 ^{ΔC/ΔC}	MF	5.0847	0.6556	7.90*

R_i , resistivity; G_i , conductance.

* WT versus AQP0^{ΔC/ΔC} DF: $P < 0.005$; WT versus AQP0^{ΔC/ΔC} MF: $P < 0.0001$.

similar to the shape of a barrel. This curvature happens because there is a decrease in the magnification of the image as the object gets farther from the center (optical axis) of the lens. The grid-focusing pattern by the AQP0^{ΔC/ΔC} lens showed an abnormal, much-distorted grid-line pattern and displayed two distinct zones. Zone I in the cortex showed a barrel distortion aberration as in the WT lenses, and zone II, at the lens nucleus, showed abnormal barrel distortion aberration compared with WT lens nucleus.

GJ Coupling in the Lenses of AQP0^{ΔC/ΔC} Mice

Aquaporins and GJ channels in the fiber cells are important components of the lens microcirculation and homeostasis. Disruption of the lens microcirculation leads to loss of lens transparency and formation of cataract.^{8,35,39,55-57} To elucidate the mechanisms by which the presence of end-cleaved AQP0, in the absence of intact AQP0, causes loss of transparency, optical distortion, and cataracts (Fig. 1) and modulates GJ channel function,¹⁷ we investigated GJ coupling conductance and HP in lenses from the mouse model AQP0^{ΔC/ΔC}.

In a previous study on age-related changes in C57 mouse lenses,⁴⁷ GJ coupling conductance and HP were measured in 3- to 5-day-old WT lenses. The MF coupling conductance was 27 Siemens per square centimeter (S/cm²) as compared to 5.2 S/cm² measured here in 10- to 13-day-old WT lenses. By 60 days of age, WT lens MF coupling has declined and pressure increased to a relatively stable value of about 0.8 S/cm² and 350 mm Hg.⁴⁷ There appears to be a rapid decline in coupling conductance during early development. If that decline is exponential, the time constant would be about 4 days. We were therefore careful to age match the WT and AQP0^{ΔC/ΔC} mouse lenses as closely as possible at 10 to 13 days. As shown in Table 1, coupling conductance per area of cell-to-cell contact of DF decreased significantly to 0.91 S/cm² ($P < 0.005$) compared to WT lenses (1.47 S/cm²). However, the coupling conductance (G_i) of MF decreased dramatically to 0.66 S/cm² compared to that of WT ($P < 0.0001$), which was 5.2 S/cm² (Table 1). These values were based on the best-fit curve (Equations 1 and 2) to R_s data shown in Figure 2. The data were collected from seven to eight lenses of each genotype. Loss of 17 amino acids at the C-terminal end of AQP0 in AQP0^{ΔC/ΔC} mice caused a significant decrease in radial coupling conductance (1.6-fold) in the DF and ~8-fold in the MF (Fig. 2; Table 1).

HP in the Lenses of AQP0^{ΔC/ΔC} Mice

The data on the radial distribution of intracellular pressure were fit with Equation 3 to determine the pressure at the lens surface ($p_i[a]$) at the transition from differentiating fiber cells to mature fiber cells ($p_i[b]$) and at the lens center ($p_i[0]$; Fig. 3; Table 2). Both $p_i(0)$ and $p_i(b)$ increased in the AQP0^{ΔC/ΔC} mouse lenses compared to WT, in line with the increased

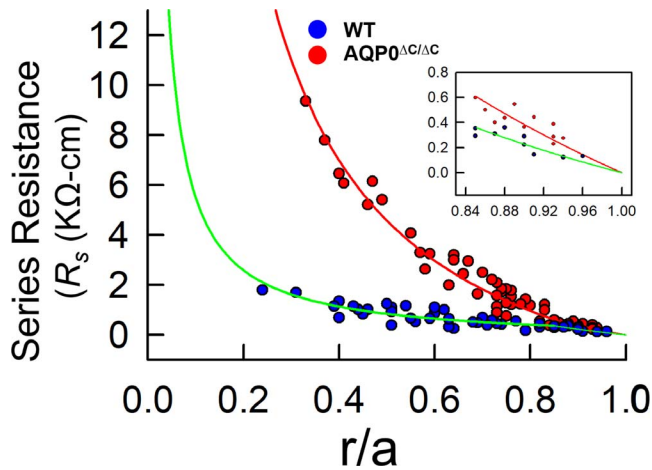


FIGURE 2. Impedance analyses of WT and AQP0^{ΔC/ΔC} lenses from P10 mouse pups. Series resistance (R_s) of lenses from WT ($n = 7$) and AQP0^{ΔC/ΔC} ($n = 8$) mice as a function of distance from lens center (r/a), where r (cm) is actual distance and a (cm) is lens radius. *Inset:* Expanded data from DF Lenses of AQP0^{ΔC/ΔC} mice pups showed a significant increase in resistance compared to WT (WT DF versus AQP0^{ΔC/ΔC} DF: $*P < 0.005$; WT MF versus AQP0^{ΔC/ΔC} MF: $*P < 0.0001$).

coupling resistance. However, $p_i(b)$ and $p_i(0)$ increased by 1.5-fold ($P < .01$) and two-fold ($P < 0.0001$), respectively, compared to the WT. The latter was significantly less than the increase in MF coupling resistance, which was about eight-fold.

In a previous study,⁴⁷ HP at the center of 3- to 5-day-old WT lenses was 62 mm Hg, so the increase in WT lens pressure between about 4 and 11 days of age was 1.6-fold, whereas the MF coupling conductance decreased from 27 S/cm² to about 5.2 S/cm², or ~5-fold. Thus, developmental changes in GJ coupling and pressure have a pattern similar to the changes in 11-day-old lenses due to the AQP0^{ΔC/ΔC} mutated lenses relative to age-matched WT lenses. Both changes involve a large decrease in MF coupling conductance accompanied by a much more modest increase in central pressure. Could the C-terminal deletion have simply accelerated normal early developmental changes? We address this question in the Discussion section, but we suspect the answer is no, since the

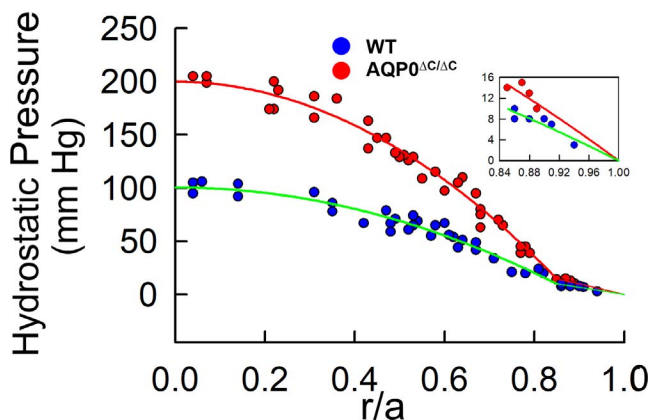


FIGURE 3. Intracellular HP in the lenses of WT and AQP0^{ΔC/ΔC} mice pups at P10. Intracellular HP in the lenses from WT and AQP0^{ΔC/ΔC} ($n = 9$) mice as a function of normalized distance from lens center (r/a). AQP0^{ΔC/ΔC} lenses show a significant increase in pressure compared to WT (WT DF versus AQP0^{ΔC/ΔC} DF: $*P < 0.01$; WT MF versus AQP0^{ΔC/ΔC} MF: $*P < 0.0001$). *Inset:* Expanded data from DF.

TABLE 2. Comparison of Intracellular HP, p_i , From P10 Lenses of WT and AQP0^{ΔC/ΔC}

Genotype	Location	p_i , mm Hg	Fold Increase
WT	$p_i(a)$	0	-
WT	$p_i(b)$	9.9889	-
WT	$p_i(0)$	100.4781	-
AQP0 ^{ΔC/ΔC}	$p_i(a)$	0	-
AQP0 ^{ΔC/ΔC}	$p_i(b)$	14.6536	1.4670*
AQP0 ^{ΔC/ΔC}	$p_i(0)$	199.6379	1.9870*

$p_i(a)$, pressure at lens surface; $p_i(b)$, pressure at the junction between DFs and MFs; $p_i(0)$, pressure in the center of the lens.

* WT versus AQP0^{ΔC/ΔC} DF: $P < 0.01$; WT versus AQP0^{ΔC/ΔC} MF: $P < 0.0001$.

mutation-induced changes lead to the rapid formation of cataracts by P15, whereas age-dependent developmental changes lead to transparent lenses that can be stable for the life of the animal.

Expression of Lens Fiber Cell Connexins in AQP0^{ΔC/ΔC} Mice

To find out whether the decreased coupling conductance observed in the AQP0^{ΔC/ΔC} lenses could be due to a decrease in GJ protein expression, we looked at the expression levels of the major lens connexins, Cx46 and Cx50. Immunoblotting of total lens membrane proteins of P10 pups of WT and AQP0^{ΔC/ΔC} mice was performed (Fig. 4). Equal quantities of the membrane proteins were immunoblotted using Cx46 and Cx50 antibodies. Western blotting and protein quantification studies showed no statistically significant difference ($P > 0.05$) in the expression levels of Cx46 or Cx50 between WT and AQP0^{ΔC/ΔC} lenses. Thus, the decreased GJ conductance and increased HP in AQP0^{ΔC/ΔC} mouse lenses indicate that C-terminal end-cleaved AQP0 expression caused either

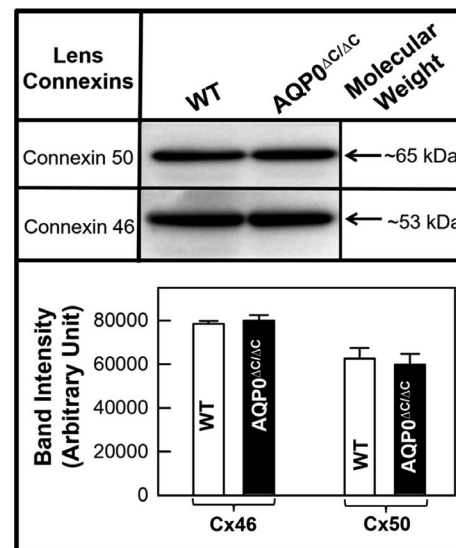


FIGURE 4. Western blotting. Total membrane proteins of WT and AQP0^{ΔC/ΔC} mice lenses at P10 showing Cx46 and Cx50 expression levels. Lens Cx46 and Cx50 proteins as recognized by their respective antibodies. Bar graphs below show a comparison of protein expression levels of Cx46 and Cx50 in the WT and AQP0^{ΔC/ΔC} mice. The protein quantification data shown in the bar graph represent mean \pm SD of five independent Western blot analyses using lenses of P10 pups from different litters.

reorganization of GJs at the membrane or reduced the open probability of GJ channels.

DISCUSSION

We investigated GJ coupling and HP in lenses expressing only end-cleaved AQP0 in their fiber cells. In a normal lens, the outer cortex contains intact AQP0; the presence of end-cleaved AQP0 begins at the inner cortex and gradually increases toward the lens center (mouse⁴⁴ and human²). Our data show a decrease in GJ coupling conductance and an increase in HP in AQP0^{ΔC/ΔC} lenses relative to age-matched WT lenses. Our studies were conducted in lenses of recently born mice (P10), since the AQP0^{ΔC/ΔC} lenses become cataractous by P15.

Newborn WT mouse lenses are undergoing rapid developmental changes.⁴⁷ At birth, GJ coupling conductance is remarkably high but rapidly declines to the adult level (estimated time constant of about 4 days). The initial high level of coupling might occur to facilitate the movement of developmental signals, such as growth factors, throughout the lens. The process, however, appears to be self-limiting, as some signal induces rapid closure of GJ channels, particularly those of the MF. The expression of AQP0^{ΔC/ΔC} instead of AQP0 appears to significantly disrupt the normal developmental program. Our data suggest the interaction of the C-terminus of AQP0 with GJs regulates coupling conductance, which appears to be one important aspect of the developmental program.

Ultrastructural studies have shown that loss of the C-terminal end of AQP0 correlates with the formation of large areas of thin junctions in WT lenses.^{14,58} GJ coupling measurements showed a significant reduction in coupling in the mature fiber cells relative to differentiating fiber cells in WT mice.^{29,31,32,34} Intracellular ion and water fluxes are both mediated by GJs,⁵³ consistent with several studies on mutant or gene knockout mouse lenses that reported a decrease/increase in GJ coupling,^{24,34,37} causing a commensurate increase/decrease in intracellular HP.^{24,34,37} In the AQP0^{ΔC/ΔC} lenses, the reduction in radial GJ conductance could be due to the formation of large areas of thin junctions from the outer cortex to the nucleus by the end-cleaved AQP0 in the fiber cells. This may have altered the formation of GJs, as observed in the WT inner cortical and nuclear regions by AFM studies.^{49,59} This reduction in GJ coupling is likely to be the cause of increased HP.

Water permeability studies using AQP0^{ΔC/ΔC} fiber cell membrane vesicles did not show any significant change;¹⁵ however, there was an increase in CTCA, possibly due to the formation of large areas of thin junctions since these lenses expressed end-cleaved AQP0 throughout.¹⁵ Normally, thin junction formation occurs at a higher level in the lens nucleus after the posttranslational N- and C-terminal cleavage of AQP0.^{49,58,59} The results presented here show that the loss of AQP0 C-terminus significantly reduces GJ coupling in both differentiating and mature fiber cells. The decrease in coupling conductance without a measurable change in connexin expression may be due to plaque reorganization in the fiber cells. However, the alternative hypothesis that there is a reduction in the open probability of GJ channels is not ruled out.

In AQP0^{ΔC/ΔC} lenses, HP is not increased nearly as much as the coupling is reduced. This pattern is similar to changes in GJ coupling and HP during normal development. However, a normal 2-month-old lens has an MF coupling conductance of 0.8 S/cm² and a central HP of 349 mm Hg,⁴⁷ whereas the AQP0^{ΔC/ΔC} lenses at 11 days of age have a MF coupling conductance of 0.7 S/cm² and a central HP of 200 mm Hg. This

implies there is less pressure-driven water flow in the AQP0^{ΔC/ΔC} lenses, so a loss of the C-terminus might cause developmental effects that reduce ion transport, leading to reduced fluid circulation in these lenses. This could be a contributing factor for the lenses developing opacities and distortion aberration (Fig. 1). However, the presence of normal AQP0 is also important for the structure of the lens, so structural distortions may contribute to opacities and distortion aberration in AQP0^{ΔC/ΔC} lenses.

A recent investigation of AQP0^{+/-} lenses expressing only 50% of AQP0 in the fiber cell membrane showed an opposite effect, with an increase in GJ conductance and a decrease in HP.²⁴ This could be due to the loss of 50% of AQP0 resulting in more surface area in the broad faces of fiber cell plasma membrane, enabling the formation of more functional GJ plaques. The presence of end-cleaved AQP0 and formation of thin junctions may be one important factor in the distribution of GJs and their radial coupling conductance.

In conclusion, GJs appear to play a critical role in early lens development. Data presented here suggest the spacial distribution of intact and C-terminal end-cleaved AQP0 from the cortex to the nucleus is critical for proper GJ channel development. Disruption of normal GJ developmental changes may cause the early onset of P15 cataracts seen in AQP0^{ΔC/ΔC} lenses.

Acknowledgments

Supported by funding from National Institutes of Health–National Eye Institute, Bethesda, Maryland, United States, Grant R01 EY026155 (KV).

Disclosure: **K. Varadaraj**, None; **J. Gao**, None; **R.T. Mathias**, None; **S. Kumari**, None

References

1. Bassnett S, Shi Y, Vrensen GF. Biological glass: structural determinants of eye lens transparency. *Philos Trans R Soc Lond B Biol Sci*. 2011;366:1250–1264.
2. Korlimbinis A, Berry Y, Thibault D, Schey KL, Truscott RJ. Protein aging: truncation of aquaporin 0 in human lens regions is a continuous age-dependent process. *Exp Eye Res*. 2009;88:966–973.
3. Kumari SS, Varadaraj K. Intact and N- or C-terminal end truncated AQP0 function as open water channels and cell-to-cell adhesion proteins: end truncation could be a prelude for adjusting the refractive index of the lens to prevent spherical aberration. *Biochim Biophys Acta*. 2014;1840:2862–2877.
4. Hall JE, Mathias RT. The aquaporin zero puzzle. *Biophys J*. 2014;107:10–15.
5. Kushmerick C, Rice SJ, Baldo GJ, Haspel HC, Mathias RT. Ion, water and neutral solute transport in *Xenopus* oocytes expressing frog lens MIP. *Exp Eye Res*. 1995;61:351–362.
6. Zampighi GA, Kremann M, Boorer KJ, et al. A method for determining the unitary functional capacity of cloned channels and transporters expressed in *Xenopus laevis* oocytes. *J Membr Biol*. 1995;148:65–78.
7. Varadaraj K, Kushmerick C, Baldo GJ, et al. The role of MIP in lens fiber cell membrane transport. *J Membr Biol*. 1999;170:191–203.
8. Shiels A, Bassnett S, Varadaraj K, et al. Optical dysfunction of the crystalline lens in aquaporin-0-deficient mice. *Physiol Genomics*. 2001;7:179–186.
9. Németh-Cahalan KL, Clemens DM, Hall JE. Regulation of AQP0 water permeability is enhanced by cooperativity. *J Gen Physiol*. 2013;141:287–295.

10. Kumari SS, Varadaraj K. Intact AQP0 performs cell-to-cell adhesion. *Biochem Biophys Res Commun.* 2009;390:1034-1039.
11. Varadaraj K, Kumari S, Mathias T. Transgenic expression of AQP1 in the fiber cells of AQP0 knockout mouse: effects on lens transparency. *Exp Eye Res.* 2010;91:393-404.
12. Kumari SS, Eswaramoorthy S, Mathias RT, Varadaraj K. Unique and analogous functions of aquaporin 0 for fiber cell architecture and ocular lens transparency. *Biochim Biophys Acta.* 2011;1812:1089-1097.
13. Liu J, Xu J, Gu S, Nicholson BJ, Jiang JX. Aquaporin 0 enhances gap junction coupling via its cell adhesion function and interaction with connexin 50. *J Cell Sci.* 2011;124:198-206.
14. Varadaraj K, Kumari SS. Molecular mechanism of Aquaporin 0-induced fiber cell to fiber cell adhesion in the eye lens. *Biochem Biophys Res Commun.* 2018;506:284-289.
15. Kumari SS, Varadaraj K. A predominant form of C-terminally end-cleaved AQP0 functions as an open water channel and an adhesion protein in AQP0^{ΔC/ΔC} mouse lens. *Biochem Biophys Res Commun.* 2018;511:626-630.
16. Bassnett S, Wilmarth PA, David LL. The membrane proteome of the mouse lens fiber cell. *Mol Vis.* 2009;15:2448-2463.
17. Varadaraj K, Kumari SS. Deletion of seventeen amino acids at the C-terminal end of aquaporin 0 causes distortion aberration and cataract in the lenses of AQP0^{ΔC/ΔC} mice. *Invest Ophthalmol Vis Sci.* 2019;60:858-867.
18. Kumari SS, Varadaraj K. Aquaporin 0 plays a pivotal role in refractive index gradient development in mammalian eye lens to prevent spherical aberration. *Biochem Biophys Res Commun.* 2014;45:986-991.
19. Kumari SS, Gupta N, Shiels A, et al. Role of aquaporin 0 in lens biomechanics. *Biochem Biophys Res Commun.* 2015;462:339-345.
20. Yu XS, Jiang JX. Interaction of major intrinsic protein (aquaporin-0) with fiber connexins in lens development. *J Cell Sci.* 2004;117:871-880.
21. Yu XS, Yin X, Lafer EM, Jiang JX. Developmental regulation of the direct interaction between the intracellular loop of connexin 45.6 and the C terminus of major intrinsic protein (aquaporin-0). *J Biol Chem.* 2005;280:22081-22090.
22. Biswas SK, Brako L, Gu S, Jiang JX, Lo WK. Regional changes of AQP0-dependent square array junction and gap junction associated with cortical cataract formation in the Emory mutant mouse. *Exp Eye Res.* 2014;127:132-142.
23. Lindsey Rose KM, Gourdie RG, Prescott AR, Quinlan RA, Crouch RK, Schey KL. The C terminus of lens aquaporin 0 interacts with the cytoskeletal proteins filensin and CP49. *Invest Ophthalmol Vis Sci.* 2006;47:1562-1570.
24. Kumari S, Gao J, Mathias RT, et al. Aquaporin 0 modulates lens gap junctions in the presence of lens-specific beaded filament proteins. *Invest Ophthalmol Vis Sci.* 2017;58:6006-6019.
25. Takemoto IJ. Quantitation of specific cleavage sites at the C-terminal region of alpha-A crystallin from human lenses of different age. *Exp Eye Res.* 1998;66:263-266.
26. Lund AL, Smith JB, Smith DL. Modifications of the water-insoluble human lens alpha-crystallins. *Exp Eye Res.* 1996;63:661-672.
27. Roy D, Spector A, Farnsworth PN. Human lens membrane: comparison of major intrinsic polypeptides from young and old lenses isolated by a new methodology. *Exp Eye Res.* 1979;28:353-358.
28. Ball LE, Garland DL, Crouch RK, Schey KL. Post-translational modifications of aquaporin 0 (AQP0) in the normal human lens: spatial and temporal occurrence. *Biochemistry.* 2004;43:9856-9865.
29. Gong, X, Baldo GJ, Kumar NM, Gilula NB, Mathias RT. Gap junctional coupling in lenses lacking alpha3 connexin. *Proc Natl Acad Sci U S A.* 1998;95:15303-15308.
30. Gong X, Agopian K, Kumar NM, Gilula NB. Genetic factors influence cataract formation in alpha 3 connexin knockout mice. *Dev Genet.* 1999;24:27-32.
31. Baldo GJ, Gong X, Martinez-Wittinghan FJ, Kumar NM, Gilula NB, Mathias RT. Gap junctional coupling in lenses from alpha(8) connexin knockout mice. *J Gen Physiol.* 2001;118:447-456.
32. White TW, Goodenough DA, Paul DL. Targeted ablation of connexin 50 in mice results in microphthalmia and zonular pulverulent cataracts. *J Cell Biol.* 1998;143:815-825.
33. White TW, Sellitto C, Paul DL, Goodenough DA. Prenatal lens development in connexin43 and connexin50 double knockout mice. *Invest Ophthalmol Vis Sci.* 2001;42:2916-2923.
34. Cheng C, Nowak RB, Gao J, et al. Lens ion homeostasis relies on the assembly and/or stability of large connexin 46 gap junction plaques on the broad sides of differentiating fiber cells. *Am J Physiol Cell Physiol.* 2015;308:C835-C847.
35. Kar R, Batra N, Riquelme MA, Jiang JX. Biological role of connexin intercellular channels and hemichannels. *Arch Biochem Biophys.* 2012;524:2-15.
36. Minogue PJ, Gao J, Zoltoski RK, et al. Physiological and optical alterations precede the appearance of cataracts in Cx46fs380 mice. *Invest Ophthalmol Vis Sci.* 2017;58:4366-4374.
37. Gao J, Minogue PJ, Beyer EC, Mathias RT, Berthoud VM. Disruption of the lens circulation causes calcium accumulation and precipitates in connexin mutant mice. *Am J Physiol Cell Physiol.* 2018;314:C492-C503.
38. Mathias RT, Kistler J, Donaldson P. The lens circulation. *J Membr Biol.* 2007;216:1-16.
39. Mathias RT, White TW, Gong X. Lens gap junctions in growth, differentiation, and homeostasis. *Physiol Rev.* 2010;90:179-206.
40. Hamann S, Zeuthen T, La Cour M, et al. Aquaporins in complex tissues: distribution of aquaporins 1-5 in human and rat eye. *Am J Physiol.* 1998;274:C1332-C1345.
41. Kumari SS, Varadaraj M, Yerramilli VS, Menon AG, Varadaraj K. Spatial expression of aquaporin 5 in mammalian cornea and lens, and regulation of its localization by phosphokinase A. *Mol Vis.* 2012;18:957-67.
42. Varadaraj K, Kumari SS, Mathias RT. Functional expression of aquaporins in embryonic, postnatal, and adult mouse lenses. *Dev Dyn.* 2007;236:1319-1328.
43. Schey KL, Wang Z, Wenke JL, Qi Y. Aquaporins in the eye: expression, function, and roles in ocular disease. *Biochim Biophys Acta.* 2014;1840:1513-1523.
44. Shiels A, Bassnett S. Mutations in the founder of the MIP gene family underlie cataract development in the mouse. *Nat Genet.* 1996;12:212-215.
45. Shiels A, Hejtmancik JF. Mutations and mechanisms in congenital and age-related cataracts. *Exp Eye Res.* 2017;156:95-102.
46. Mathias RT, Rae JL, Baldo GJ. Physiological properties of the normal lens. *Physiol Rev.* 1997;77:21-50.
47. Gao J, Wang H, Sun X, et al. The effects of age on lens transport. *Invest Ophthalmol Vis Sci.* 2013;54:7174-7187.
48. Gao J, Sun X, White TW, Delamere NA, Mathias RT. Feedback regulation of intracellular hydrostatic pressure in surface cells of the lens. *Biophys J.* 2015;109:1830-1839.
49. Buzhynskyy N, Sens P, Behar-Cohen F, Scheuring S. Eye lens membrane junctional microdomains: a comparison between healthy and pathological cases. *New J Phys.* 2011;13:085016.

50. Buzhynskyy N, Girmens JF, Faigle W, Scheuring S. Human cataract lens membrane at subnanometer resolution. *J Mol Biol.* 2007;374:162-169.
51. Kumari SS, Gandhi J, Mustehsan MH, Eren S, Varadaraj K. Functional characterization of an AQP0 missense mutation, R33C, that causes dominant congenital lens cataract, reveals impaired cell-to-cell adhesion. *Exp Eye Res.* 2013;116:371-385.
52. Alizadeh A, Clark J, Seeberger T, Hess J, Blankenship T, FitzGerald PG. Characterization of a mutation in the lens-specific CP49 in the 129 strain of mouse. *Invest Ophthalmol Vis Sci.* 2004;45:884-891.
53. Gao J, Sun X, Moore LC, White TW, Brink PR, Mathias RT. Lens intracellular hydrostatic pressure is generated by the circulation of sodium and modulated by gap junction coupling. *J Gen Physiol.* 2011;137:507-520.
54. Mathias RT, Rae JL, Eisenberg RS. The lens as a nonuniform spherical syncytium. *Biophys J.* 1981;34:61-83.
55. Zampighi GA, Kreman M, Boorer KJ, et al. A method for determining the unitary functional capacity of cloned channels and transporters expressed in *Xenopus laevis* oocytes. *J Membr Biol.* 1995;148:65-78.
56. Gao J, Sun X, Martinez-Wittinghan FJ, Gong X, White TW, Mathias RT. Connections between connexins, calcium, and cataracts in the lens. *J Gen Physiol.* 2004;124:289-300.
57. Martinez-Wittinghan FJ, Sellitto C, White TW, Mathias RT, Paul D, Goodenough DA. Lens gap junctional coupling is modulated by connexin identity and the locus of gene expression. *Invest Ophthalmol Vis Sci.* 2004;45:3629-3637.
58. Zampighi GA, Eskandari S, Hall JE, Zampighi L, Kreman M. Micro-domains of AQP0 in lens equatorial fibers. *Exp Eye Res.* 2002;75:505-519.
59. Scheuring S, Buzhynskyy N, Jaroslowski S, Goncalves RP, Hite RK, Walz T. Structural models of the supramolecular organization of AQP0 and connexons in junctional microdomains. *J Struct Biol.* 2007;160:385-394.